Available online at www.sciencedirect.com
SCIENCE DIRECT®
International Journal of Refrigeration 27 (2004) 940–947
REVUE INTERNATIONALE DU FROID
INTERNATIONAL JOURNAL OF
refrigeration
www.elsevier.com/locate/ijrefrig

Experimental pure fluid and binary mixture performance in a heat pump equipped with a distillation column

James G. Gebbie[a,*], Michael K. Jensen[a], Piotr A. Domanski[b], David A. Didion[b]

[a]*Department of Mechanical, Aerospace, and Nuclear Engineering, Rensselaer Polytechnic Institute, Troy, NY 12180-3590, USA*
[b]*National Institute of Standards and Technology, Gaithersburg MD 20899-8631, USA*

Received 18 July 2003; received in revised form 13 April 2004; accepted 6 May 2004

Abstract

An experimental heat pump system that included a distillation column, accumulator/sump, and heater was experimentally investigated using two different working fluids, R32 and a mixture of R32/134a. Performance variations with changes in sump heater power, condenser and evaporator heat transfer fluid flow, and compressor speed were examined. Heating capacity generally increased with increases in the factors tested. Heating capacity increases were generally smaller with the R32/134a tests than with the R32 tests, except with variations in sump heater power. An increase in sump heater power caused a pronounced increase in the circulating R32 concentration during the mixture tests, and the heating capacity increased markedly. The increase in heating capacity with sump heater power during the R32/134a tests was on par with the increase with compressor power during these same tests. The increase in capacity with sump heater power during the R32/134a tests also was substantial even when compared with the capacity increase with compressor speed during the R32 tests.

Keywords: Design; Heat pump; Distillation; Experiment; Binary mixture R-32; R-134a

Performance expérimentale des frigorigères purs et des mélanges binaires utilisés dans une pompe à chaleur munie d'une colonne à distillation

Mots-clé: Conception; Pompe à chaleur; Distillation; Expérimentation; Mélange binaire; R-32; R-134a

1. Introduction

Ozone depletion, global warming, and efficient energy usage have been the primary motivations for recent vapor-compression-cycle heat pump research. The need for alternatives to traditional CFC and HCFC refrigerants (e.g., R22) has led to consideration of refrigerant mixtures as replacement alternatives. In addition to replacing environmentally damaging pure fluid refrigerants, zeotropic mixtures present potential thermodynamic cycle advantages.

The first advantage of using a zeotropic mixture in a vapor-compression-cycle heat pump is related to the glide-temperature-difference (GTD). As a zeotropic mixture transitions from one phase to another, the temperature of the mixture changes. In a condenser and/or an evaporator, if the refrigerant temperature glide is matched to the heat transfer fluid (HTF) temperature glide due to sensible heat change, then the effective temperature difference between the refrigerant and HTF can be reduced (Fig. 1). Mulroy

* Corresponding author. Tel.: +1-248-650-1130.
E-mail address: gebbij@earthlink.net (J.G. Gebbie).

0140-7007/$ - see front matter © 2004 Elsevier Ltd and IIR. All rights reserved.
doi:10.1016/j.ijrefrig.2004.05.003

Nomenclature

COP	coefficient of performance (–)
c_{p_f}	constant pressure specific heat of the HTF (J/kg K)
EOT	end of test (–)
GTD	glide temperature difference (–)
HTF	heat transfer fluid (–)
$\hat{M}_i$	molar mass of component i (g/mol)
$\dot{m}_{cd}$	HTF mass flow rate through the condenser (kg/s)
$\dot{m}_{ev}$	HTF mass flow rate through the evaporator (kg/s)
$\dot{m}_f$	HTF mass flow rate (kg/s)
$\dot{q}_{cd}$	condenser heat transfer rate/capacity (W)
$\dot{q}_{ev}$	evaporator heat transfer rate/capacity (W)
$\dot{q}_{sp}$	sump heater input power (W)
rpm_{cp}	compressor speed (revolutions/min)
s	entropy (kJ/kg °C)
T	temperature (°C)
$T_{f,cd}$	HTF temperature in the condenser (°C)
$T_{f,ev}$	HTF temperature in the evaporator (°C)
$T_{f_{in}}$	heat exchanger HTF inlet temperature (°C)
$T_{f_{out}}$	heat exchanger HTF outlet temperature (°C)
$T_{r,cd}$	refrigerant temperature in the condenser (°C)
$T_{r,ev}$	refrigerant temperature in the evaporator (°C)
τ_{cp}	compressor shaft torque (N m)
$\dot{w}_{cp}$	compressor power (W)
z_{sample}	R32 mass fraction of the sample analyzed by the gas chromatograph (–)

et al. [1] and Domanski et al. [2] demonstrated that 'glide matching' tends to decrease irreversible heat transfer and increase the coefficient of performance (COP).

The second advantage of using zeotropic mixtures is that changing the overall composition of the circulating refrigerant can modulate heating capacity. Cooper and Borchart [3] and Gromoll and Gutbier [4] showed that increasing the volatility of the circulating refrigerant will tend to increase heating capacity. If heating capacity is increased when the outdoor air temperature is below where capacity matches load ('balance point,' Fig. 2), then less

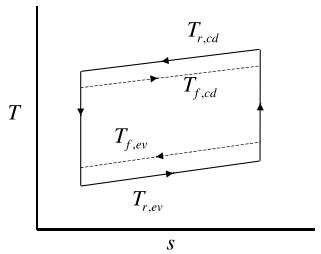

Fig. 1. Glide matching of refrigerant and HTF temperature profiles.

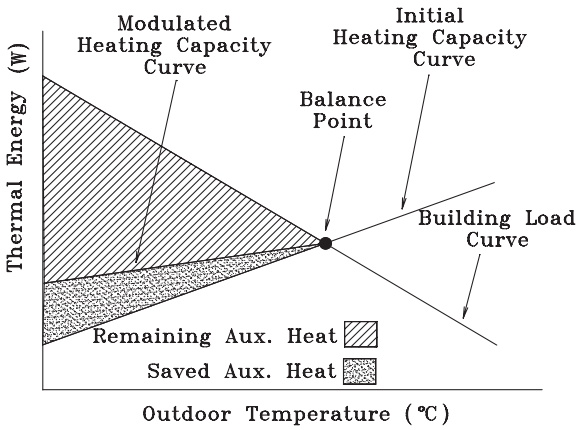

Fig. 2. Building load/capacity modulation benefit.

auxiliary heating is needed. Electrical resistance heat, which has a COP of unity, is often used to supply the additional demand. Therefore, increasing heat pump capacity at lower ambient temperatures benefits electrical customers and reduces peak electrical demand.

Rothfleisch [5] experimentally showed that when a heat pump was charged with a refrigerant mixture, decreasing outdoor air temperature shifted the circulating refrigerant composition toward the more volatile component, and the less volatile component was preferentially stored as liquid in the accumulator. Consequently, the capacity decrease with outdoor air temperature was attenuated because the refrigerant in the evaporator could absorb heat more easily. Rothfleisch also showed that a properly placed distillation column (along with an additional heat source) could be used to enhance the composition shift and further attenuate the capacity decrease.

The type of refrigerant used in a heat pump is only one of several design parameters. Others include the compressor displacement, compressor speed, heat exchanger sizing, and so on. However, work, comparing composition shifting with other design parameters was not found in the open literature. The goal of the present investigation was to experimentally examine performance variations due to composition shifting in the context of a modest list of design parameter variations. The experimental system was of a similar design to Rothfleisch [5] so that distillation parameters could be included in the investigation.

2. Experimental apparatus and procedures

The distillation heat pump (DHP) system constructed for this research consisted of a vapor compression cycle loop and two water–ethylene glycol HTF loops (Fig. 3). A variable-speed reciprocating compressor was used to pump the refrigerant. The condenser and evaporator were counter-flow heat exchangers and each was composed of annular tubes. Refrigerant flowed through the center tube and the

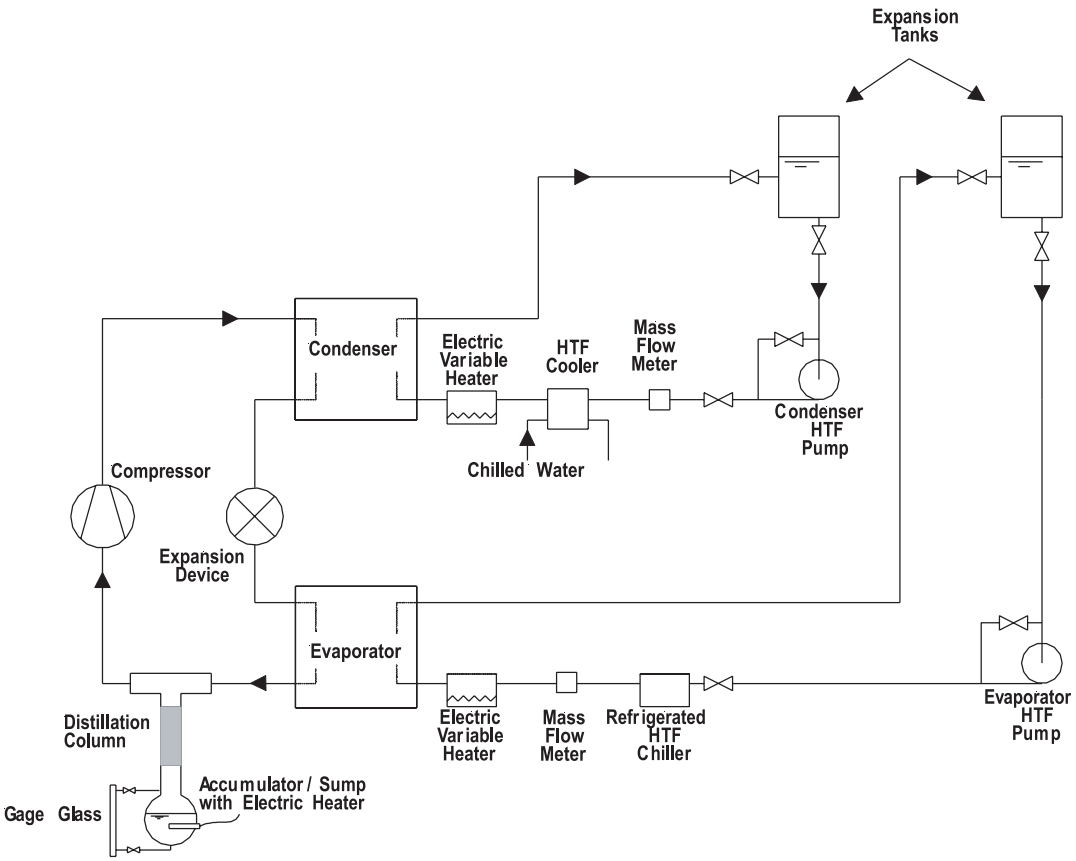

Fig. 3. Experimental distillation heat pump.

HTF flowed through the finned annular portion. A more detailed description of the heat exchangers may be found in Refs. [6,7]. The expansion device was a needle valve. A distillation column, refrigerant storage accumulator, and electrical heat source were incorporated into the refrigerant loop in the manner prescribed by Rothfleish [5]. In fact, the column was the same as that used by Rothfleish and design details for that column may be found in the cited reference.

The distillation accumulator sump was constructed from a copper pipe. The sump volume was approximately 5 l, and the level inside was monitored using a gage-glass. An electrically powered cartridge heater, to generate vapor for the distillation column, was mounted in the bottom of the sump.

Ten ports were provided on the compressor discharge line for sampling refrigerant. Samples were drawn from this location to ensure that the refrigerant was a single-phase vapor, as required for sample analysis by gas chromatography.

A turbine pump provided flow through each HTF loop, and elevated 'flow-through' expansion tanks were installed in each HTF loop. Each expansion tank served as a surge volume, provided pump suction head and, because HTF flowed through them, a simple means of adjusting HTF thermal mass. Flow rates through the HTF loops were measured using Coriolis effect flow meters.

HTF inlet temperatures to the condenser and evaporator were controlled by overcooling, using chilled water in the condenser HTF loop and an R134a chiller unit in the evaporator loop, then re-heating using variable electric immersion heaters.

Temperature measurements throughout the system were made using type-T thermocouples. Thermopiles, consisting of 10 type-T thermocouples immersed directly in the HTF, were used to measure sensible heat change across the heat exchangers.

Two working fluids were used. The first was R32 and the second was a 30/70% by mass mixture of R32/134a. A full factorial design [8] experiment with two levels per factor was used for each fluid. The four independent variables tested were: sump heater input power, evaporator HTF mass flow rate, condenser HTF mass flow rate, and compressor speed.

The factorial design required that each independent variable (i.e., factor) have two settings. The low/high sump heater power, condenser and evaporator HTF mass flow, and compressor speed settings were 25/100 W, 0.08/0.16 kg/s, and 800/1000 rpm, respectively. The values of these settings

were chosen as a result of preliminary system tests using R134a [9]. Each set of 16 tests (one set per fluid) was conducted in random order to minimize hysteresis.

All tests were performed at a low evaporator HTF inlet temperature heating condition, a moderate room ambient condenser HTF inlet temperature, and with the same charged mass of R32. The nominal evaporator HTF inlet temperature, condenser HTF inlet temperature, and R32 charge were −7 °C, 20 °C, and 1500 g, respectively.

Ideally, experiments of this sort would be run until the system reached steady state and the results would be reported as such. However, transient testing with this system [10] showed that, particularly when charged with a refrigerant mixture, 'steady state' was difficult to identify. The typical indicators: rates of system change and system energy balance were not dependable. For this reason, data for each test were obtained after the system was placed in a reliably repeatable initial condition and run for the same duration (1 h).

The heat pump was operated at the conditions to be tested until the capacity and sump level were relatively steady. The heat pump was then shut down with the HTFs still flowing and the heat exchanger HTF inlet temperatures maintained constant. The compressor was intermittently 'jogged' to pump as much liquid refrigerant as possible to the sump. After jogging the refrigerant into the sump, the compressor was started, and performance data obtained after one hour. This 'one hour' data set is referred to as the end-of-test (EOT) data. It is not described as steady state because the system had not reached equilibrium during some of the tests.

Some of the data to be reported from this work were read directly from the instrumentation used (e.g., sump heater power, sump liquid level, and compressor speed), while others required supplemental calculations. Details can be found in Ref. [10].

With the torque and speed of the compressor shaft available from the transducer data, compressor power was calculated using

$$\dot{w}_{cp} = \tau_{cp} \mathrm{rpm}_{cp} \tag{2}$$

The heat exchanger capacity calculations were based on the sensible heat change and mass flow of the HTF.

$$\dot{q} = \dot{m}_f c_{p_f} (T_{f_{out}} - T_{f_{in}}) \tag{3}$$

The temperature differences were measured by the thermopiles across each heat exchanger.

COPs were calculated using

$$\mathrm{COP} = \frac{\dot{q}_{cd}}{\dot{w}_{cp} + \dot{q}_{sp}} \tag{4}$$

The sump heater power is included in the denominator of Eq. (4) so that the tradeoff between an increase in sump heater power and increased system performance could be easily evaluated.

A thermal conductivity type gas chromatograph was used to determine the mass fractions of the constituents in the refrigerant samples. Reference data were obtained from an analysis of each pure fluid.

The root-mean-squared (RMS) uncertainty [11] and experimental repeatability of the data were examined. The uncertainties in condenser and evaporator capacities, and compressor power were found to be ±1.5%. The uncertainty in COP was ±2%. The uncertainty in R32 mass fraction in an R32/134a mixture was found to be ±0.5% by mass R32. The experimental repeatability in condenser capacity, compressor power, and COP were ±1%, and the repeatability in evaporator capacity was ±2.5%.

The uncertainty and repeatability of the independent variables ($\dot{q}_{sp}$, $\dot{m}_{cd}$, $\dot{m}_{ev}$, and rpm_{cp}) and nominally constant HTF inlet temperatures were also examined. The uncertainty in sump heater power was ±0.5%, and the uncertainty in the HTF flow rates for both heat exchangers was ±0.15%. The uncertainty in the HTF inlet temperatures was ±1 °C. The compressor speed data were considered to be exact because the readings were derived directly from a rotation counter. The repeatability of the sump heater power was ±9% at 25 W and ±5% at 100 W. Condenser mass flow was repeatable to within ±1.5% over all the data, and the evaporator mass flow repeatability was ±6%. The experimental repeatability of the compressor speed was ±2.5%. Details of the RMS analysis and experimental uncertainty determination can be found in Ref. [10].

3. Results

The performance results at each nominal factor setting (in terms of primitive variables) are presented in Tables 1(a) and (b).

To compare the data, the mean condenser capacity, mean evaporator capacity, and compressor power changes due to increases in each factor, normalized by the overall mean, are presented in Figs. 4–6, respectively. For example, referring to Table 1(a), eight tests were conducted with R32 at the low sump heater power setting, and eight were conducted at the high setting. The average percent change in the condenser capacity due to the increase in sump heater power was calculated using

$$\%\langle \Delta \dot{q}_{cd} \rangle_{\dot{q}_{sp}} = \frac{\frac{1}{8}\sum_{i=1}^{8} (\dot{q}_{cd_i}|_{\text{tests in which } \dot{q}_{sp}=100\text{ W}} - \dot{q}_{cd_i}|_{\text{tests in which } \dot{q}_{sp}=25\text{ W}})}{\langle \dot{q}_{cd} \rangle} 100 \tag{5}$$

The average changes in circulating R32 concentration (% by mass) with due to each factor are presented in Fig. 7. These were calculated in a similar manner to Eq. (5), but without normalization and without multiplying by 100.

In order to compare the factorial variations of the

Table 1a
Primitive R32 EOT results

Nominal factor settings				EOT results				
$\dot{q}_{sp}$ (W)	$\dot{m}_{ev}$ (kg/s)	$\dot{m}_{cd}$ (kg/s)	rpm_{cp} (rev./min.)	$\dot{q}_{cd}$ (W)	$\dot{q}_{ev}$ (W)	$\dot{w}_{cp}$ (W)	COP	R32 % by mass
25	0.08	0.08	800	1887	1342	490	3.66	100
100	0.08	0.08	800	1891	1282	490	3.19	100
25	0.16	0.08	800	2058	1553	516	3.80	100
100	0.16	0.08	800	2098	1462	511	3.43	100
25	0.08	0.16	800	1947	1390	486	3.81	100
100	0.08	0.16	800	1940	1309	486	3.31	100
25	0.16	0.16	800	2114	1562	489	4.10	100
100	0.16	0.16	800	2171	1538	499	3.62	100
25	0.08	0.08	1000	2245	1624	627	3.44	100
100	0.08	0.08	1000	2271	1564	636	3.08	100
25	0.16	0.08	1000	2520	1853	661	3.67	100
100	0.16	0.08	1000	2567	1840	665	3.36	100
25	0.08	0.16	1000	2347	1653	605	3.72	100
100	0.08	0.16	1000	2372	1620	621	3.28	100
25	0.16	0.16	1000	2608	1987	638	3.93	100
100	0.16	0.16	1000	2644	1862	642	3.56	100

R32/134a data with those from the R32 tests, the average increase in the R32/134a performance variables as a percentage of the same variables from the R32 tests were examined. Again, using the condenser capacity variations with sump heater power as an example

$$\left\langle \frac{\dot{q}_{cd}|_{\text{R32/134a tests}}}{\dot{q}_{cd}|_{\text{R32 tests}}} \right\rangle_{\text{tests in which } \dot{q}_{sp}=100\text{ W}} = \frac{100}{8}\sum_{i=1}^{8} \frac{\dot{q}_{cd_i}|_{\text{R32/134a tests in which } \dot{q}_{sp}=100\text{ W}}}{\dot{q}_{cd_i}|_{\text{R32 tests in which } \dot{q}_{sp}=100\text{ W}}} \quad (6)$$

The results of using Eq. (6) for condenser capacity and COP over all of the factors are shown in Fig. 8.

During the R32 tests, condenser capacity was relatively unchanged by an increase in sump heater power. The increased energy input to the sump was offset by a decrease in that absorbed by the evaporator (Fig. 5). At fixed compressor speed, HTF flow rates, and refrigerant composition (pure R32 in this case), the ability of the system to absorb energy on the low-side and reject it on the high-side was fairly constant. Note that the compressor power (Fig. 6) was not significantly

Table 1b
Primitive R32/134a EOT results

Nominal factor settings				EOT results				
$\dot{q}_{sp}$ (W)	$\dot{m}_{ev}$ (kg/s)	$\dot{m}_{cd}$ (kg/s)	rpm_{cp} (rev./min.)	$\dot{q}_{cd}$ (W)	$\dot{q}_{ev}$ (W)	$\dot{w}_{cp}$ (W)	COP	R32 % by mass
25	0.08	0.08	800	1534	1106	389	3.70	59.9
100	0.08	0.08	800	1774	1261	450	3.22	84.7
25	0.16	0.08	800	1673	1280	412	3.83	67.9
100	0.16	0.08	800	1949	1424	472	3.41	85.5
25	0.08	0.16	800	1645	1170	390	3.96	64.4
100	0.08	0.16	800	1850	1292	435	3.45	83.8
25	0.16	0.16	800	1628	1235	394	3.89	62.5
100	0.16	0.16	800	1994	1430	443	3.67	80.3
25	0.08	0.08	1000	1966	1411	525	3.57	71.4
100	0.08	0.08	1000	2096	1442	562	3.17	85.1
25	0.16	0.08	1000	1930	1441	506	3.63	62.1
100	0.16	0.08	1000	2239	1635	584	3.28	74.2
25	0.08	0.16	1000	1880	1356	486	3.67	61.7
100	0.08	0.16	1000	2069	1428	531	3.27	73.4
25	0.16	0.16	1000	1905	1394	481	3.76	61.5
100	0.16	0.16	1000	2090	1462	522	3.35	61.0

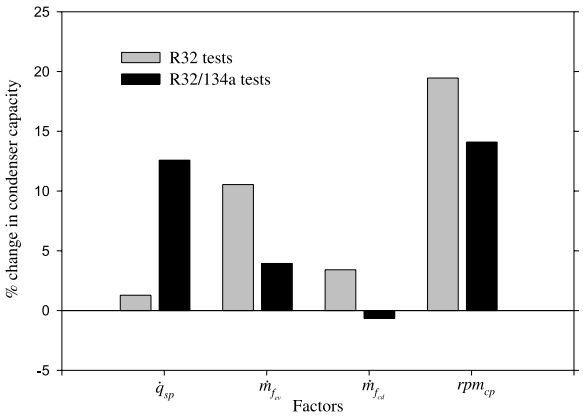

Fig. 4. Factorial percent changes in condenser capacity.

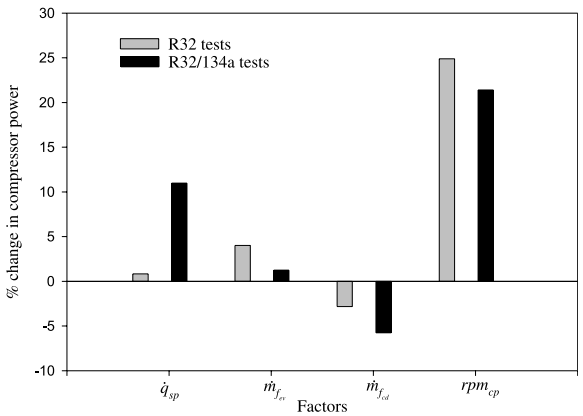

Fig. 6. Factorial percent changes in compressor power.

changed by increased sump heater power during the R32 tests.

During the R32/134a tests, an increase in sump heater power increased condenser capacity an average of 13% (Fig. 4). Fig. 5 shows that the energy absorbed in the evaporator increased an average of 9% with sump heater power, and the compressor power increased 11% (Fig. 6). The increased heat absorption was a result of the distillation column increasing the R32 concentration (Fig. 7) and, therefore, the volatility of the circulating refrigerant. Fig. 8 shows that an increase in sump heater power increased the average R32/134a condenser capacity from 80% of the R32 value to 90%. The average COP during R32/134a tests was 100% of the R32 value at both factor settings (Fig. 8).

On average, the increase in evaporator HTF flow increased condenser capacity 11% during the R32 tests (Fig. 4). This was due to a 15% increase in evaporator capacity (Fig. 5), which, in turn, was due to an increased average temperature difference between the HTF and the refrigerant, and the decrease in heat transfer resistance on the HTF side of the evaporator. There was also a 3% increase in compressor power input (Fig. 7).

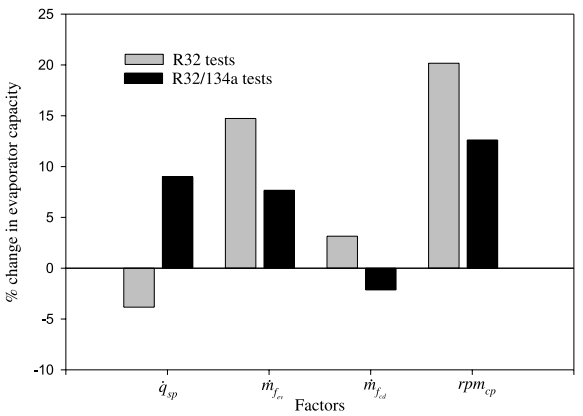

Fig. 5. Factorial percent changes in evaporator capacity.

Condenser capacity increased by 3%, evaporator capacity increased by 8%, and compressor power increased by 1% with increased evaporator HTF flow during the R32/134a experiments (Figs. 4–6, respectively). The energy absorption increase in the evaporator and subsequent rejection in the condenser was less substantial than during the R32 tests due to decreased circulating R32 concentration (Fig. 7). The authors hypothesize that increased evaporator HTF flow tended to decrease the quality of the refrigerant leaving the evaporator, and the additional liquid refrigerant, richer in R134a, was separated into the sump. Thus, R134a concentration in the sump increased. As the sump was the source of vapor for the distillation column, this caused a decrease in R32 concentration through out the system. Fig. 8 shows that the R32/134a condenser capacity decreased from 87% to 82% of the R32 value with evaporator HTF flow. COP of the R32/134a tests also decreased slightly from 102% of the R32 value at the low HTF setting to 98% at the higher setting.

The decrease in heat transfer resistance on the HTF side along with the increased average temperature difference

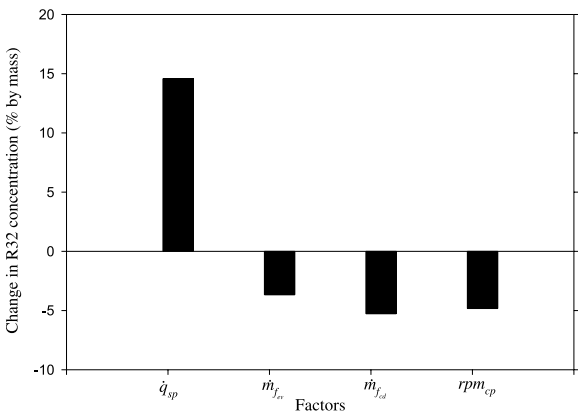

Fig. 7. Factorial changes in circulating R32 concentration during R32/134a tests.

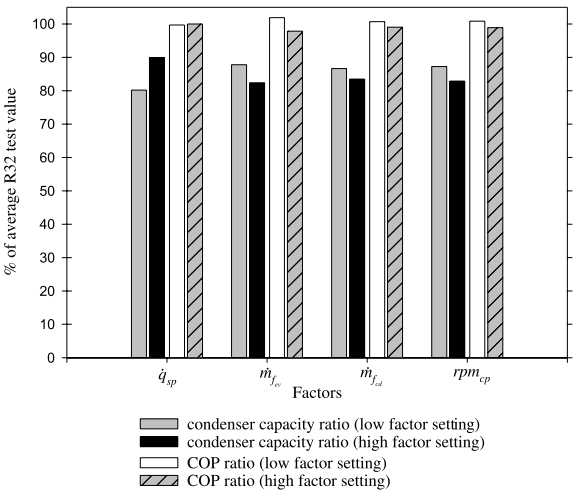

Fig. 8. Performance comparison between R32 and R32/134a tests.

between the HTF and refrigerant in the condenser with increased condenser HTF flow increased the condenser and evaporator capacities by 3%, and decreased the compressor power by 3% (Figs. 4–6, respectively). Fig. 6 shows that condenser HTF flow was the only factor whose increase caused a decrease in compressor power. This is reasonable because the decreased heat transfer resistance in the HTF allowed lower saturation pressures on the high-side (hence, lower compression ratios) for a given capacity, and the capacity increase with HTF flow was small (Fig. 4).

Increased condenser HTF flow did not significantly change condenser capacity during the R32/134a tests (<1%, Fig. 4). Evaporator capacity decreased slightly (2%, Fig. 5) and compressor power decreased by 6% (Fig. 6). Fig. 7 shows that circulating R32 concentration decreased an average of 6% during the R32/134a tests. This was the reason for the decreased heat absorption in the evaporator. Decreased heat absorption, due to lower volatility, and a more substantial decrease in compressor power (6% versus 3%, Fig. 6) were the reasons that condenser capacity remained unchanged instead of increasing as it did during the R32 tests. Increasing the condenser HTF flow decreased the R32/134a condenser capacity from 87% to 83% of the R32 capacity (Fig. 8). The relative COP decrease shown in Fig. 8 (101 to 100%) was not significant in light of the measurement uncertainty.

Increasing compressor speed increased condenser and evaporator capacities and compressor power in direct proportion (19, 20, 25%, Figs. 4–6, respectively) to the speed increase (20%). The proportionality of the compressor power increase was somewhat surprising in light of pump laws that generally suggest a cubic relationship between pump speed and power. However, density and compression ratio variations conspired to make the power increase closer to linear with speed in this case.

The increase in condenser and evaporator capacity with compressor speed was 14% and 13% (Figs. 4 and 5, respectively) during the R32/134a tests. This was substantially less than the capacity increases during the R32 tests; yet, the percent compressor power increase was nearly the same (21% compared with 25%, Fig. 6). The reason for the smaller capacity increase was the decrease in circulating R32 concentration (Fig. 7). The associated decrease in circulating refrigerant volatility decreased the ability to absorb heat in the evaporator without decreasing the 'cost' (increased compressor power). Increasing compressor speed decreased the R32/134a capacity from 87% of the R32 value to 83%. The relative COP decrease was, again, not significant (101 to 99%, Fig. 8).

4. Conclusions

An experimental investigation was conducted into the effects of using either a refrigerant mixture (30/70% by mass R32/134a) or a pure fluid (R32) on heat pump performance. The work was motivated by improved energy utilization, and the need to examine system effects in the context of a variety of parametric changes. Due to its potential for enhancing composition changes when a heat pump is charged with a zeotropic mixture, a distillation column was installed in the manner prescribed by Rothfleisch [5].

The data obtained show that increased sump heater power, HTF flow, and compressor speed will all modulate the heating capacity of a heat pump. However, the capacity increases during the R32/134a tests with increased HTF flow and compressor speed were always less than those of the R32 tests. Also, capacity modulation using these two mechanisms would likely require different motors for the driving devices (fans and compressors in systems used in the field) in addition to a modest control system to provide for load following.

During the R32/134a tests, increased sump heater power produced an average capacity increase that was greater than those produced by increased HTF flow during either the R32 tests or the R32/134a tests. Furthermore, the increase was quite close to that obtained by increasing compressor speed during the R32/134a tests (13% versus 14%, Fig. 8) and respectable compared to the capacity increase with compressor speed during the R32 tests (13% versus 19%). The increases were dependent on the levels of the factors chosen, but the degree of capacity increase with a modest (75 W) increase in sump heater power was impressive compared with compressor speed.

Rothfleish [5] has suggested that a source of sump heat internal to the heat pump system (e.g., liquid-line heat) could be used in place of an externally powered heater. In addition to removing the need for the heater, and modestly improving the COP (Eq. (5)), this would lead to the intriguing possibility of passive load following. That is, if

the heat transfer rate to the sump varied with the outdoor temperature, then the heat pump capacity could be varied by altering the circulating composition without an external control system.

Acknowledgements

The National Institute of Standards and Technology (NIST) sponsored the research presented here as part of its continuing efforts to work with industry and improve energy utilization. Their financial support, in addition to their facilities and expertise, is gratefully acknowledged.

References

[1] Mulroy WJ, Domanski PA, Didion DA. Glide matching with binary and ternary zeotropic refrigerant mixtures part 1. An experimental study. Int J Refrigeration 1994;17(4):220–5.
[2] Domanski PA, Mulroy WJ, Didion DA. Glide matching with binary and ternary zeotropic refrigerant mixtures part 2. A computer simulation. Int J Refrigeration 1994;17(4):226–30.
[3] Cooper WD, Borchardt HJ. The use of refrigerant mixtures in air-to-air heat pumps. XVth International Congress of Refrigeration, Proceedings 1979;4:995–1001.
[4] Gromoll B, Gutbier H. Continuous control of the heating capacity of heat pumps by means of non-azeotropic mixtures. Proceedings of Commision E2 of the International Institute of Refrigeration, Trondheim, Norway 1985;257–63.
[5] Rothfleisch PI. A simple method of composition shifting with a distillation column for a heat pump employing a zeotropic refrigerant mixture. NISTIR 5689, Gaithersburg, MD: National Institute of Standards and Technology; 1995.
[6] Kedzierski MA, Kim MS. Single-phase heat transfer and pressure drop characteristics of an integral-spine-fin within an annulus. NISTIR 5454, Gaithersburg, MD: National Institute of Standards and Technology; 1994.
[7] Kedzierski MA, Kim MS. Convective boiling and condensation heat transfer with a twisted-tape insert for R12, R22, R152a, R134a, R290, R32/R134a, R32/152a, R290/R134a, R134a/R600a. NISTIR 5905, Gaithersburg, MD: National Institute of Standards and Technology; 1997.
[8] Ott L. An introduction to statistical methods and data analysis. Boston, MA: PWS-Kent Publishing Co; 1988.
[9] Gebbie JG, Jensen MK. Development and verification of a simulation model of a zeotropic refrigerant mixture heat pump with a distillation column. Progress Report Prepared Under NIST Purchase Order #43NANB714532, Gaithersburg, MD: National Institute of Standards and Technology; 1998.
[10] Gebbie JG. Pure fluid and binary mixture transients of a heat pump equipped with a distillation column: an experimental and numerical investigation. PhD Thesis, Rensselaer Polytechnic Institute, Troy, NY; 2002.
[11] Moffat RJ. Describing the uncertainties in experimental results. Exp Therm Fluid Sci 1988;1(1):3–17.